

Heterogenized iron(II) complexes as highly active ethene polymerization catalysts

Roland Schmidt^a, M. Bruce Welch^b, Syriac J. Palackal^b, Helmut G. Alt^{a,*}

^a *Laboratorium für Anorganische Chemie, Universität Bayreuth, Postfach 10 12 51, D-95440 Bayreuth, Germany*

^b *Phillips Petroleum Company, Research and Development Center, 74004 Bartlesville, OK, USA*

Received 5 April 2001; accepted 16 August 2001

Abstract

The synthesis of new iron(II) diiminopyridine complexes and their heterogenization to give highly active ethene polymerization catalysts is described. The ligands are characterized by ¹H NMR, ¹³C NMR spectroscopy and GC/MS. The complexes are paramagnetic and were characterized by elemental analyses and mass spectrometry. The complexes were activated and heterogenized with a cocatalyst consisting of partially hydrolyzed trimethylaluminum (PHT) on silica gel and were used for ethene polymerization.

The polymerization results and the polymer properties are presented. The influence of the catalyst structure, hydrogen and 1-hexene on the polymerization behavior is discussed. © 2002 Elsevier Science B.V. All rights reserved.

Keywords: Iron(II) complexes; Catalysis; Heterogenization; Ethene polymerization; Polymer properties

1. Introduction

In 1998, Small et al. [1], and Britovsek et al. [2–5] independently described olefin polymerization and oligomerization catalysts prepared by reacting a well-known class of compounds [6], diiminopyridine complexes of iron and cobalt, with an activator such as methylaluminoxane (MAO) [7–11]. Unfortunately, these homogeneous catalysts require a large excess of expensive MAO when used to oligomerize and/or polymerize ethene and result in reactor fouling in slurry processes. For these reasons, these homogeneous catalysts are unattractive for industrial applications. In general, reactor fouling can be avoided in the slurry loop process by making catalysts heteroge-

neous. Metallocene catalysts can be made heterogeneous by either immobilizing the catalyst precursor or the cocatalyst. An efficient way of immobilizing the cocatalyst is to precipitate the MAO on a carrier material [12–15]. The catalyst precursor is then added to the immobilized MAO to form the activated catalyst.

A common way of immobilizing MAO consists of depositing it on the surface of silica. Some of the resulting ‘solid MAO’ are commercially available. A significant disadvantage in using these materials is an associated decrease in activity.

To overcome the disadvantages of homogeneous and ‘solid MAO’ polymerizations, we prepared partially hydrolyzed trimethylaluminum (PHT), a solid formed by reacting a carrier and trimethylaluminum (TMA) with water for the activation of new diiminopyridine complexes of iron(II). The resulting catalysts were used for ethene polymerization.

* Corresponding author. Tel.: +49-921-552555;

fax: +49-921-552157.

E-mail address: helmut.alt@uni-bayreuth.de (H.G. Alt).

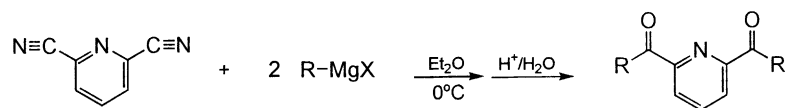


Fig. 1. Synthesis of diketones.

2. Results and discussion

2.1. Preparation of the ligand precursor

The common starting compound for the syntheses of the desired tridentate ligands is 2,6-dicyanopyridine. This pyridine is reacted with the appropriate Grignard reagent in diethylether and subsequently treated with dilute sulfuric acid to yield the corresponding diketone (Fig. 1).

2.2. Synthesis of the compounds 1–16

The diketone is reacted with a suitable aniline in a condensation reaction (Schiff's base reaction [6]) to give the corresponding diiminopyridine compounds **1–16** (Fig. 2).

2.3. Characterization of compounds 1–16

Compounds **1–16** were prepared in accordance with the procedure shown in Fig. 2 and analyzed via ^1H

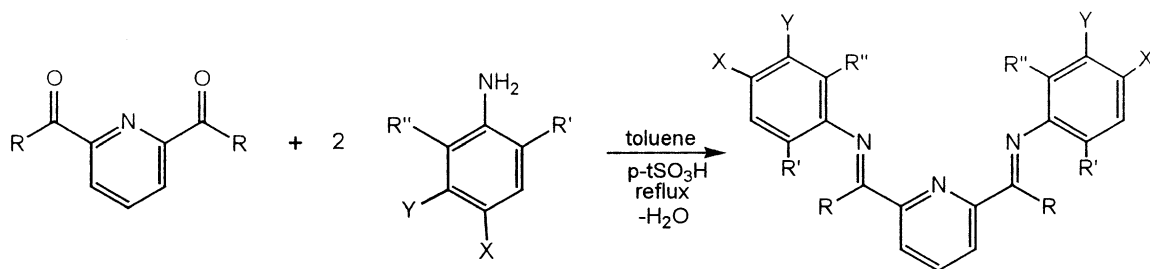
NMR and ^{13}C NMR spectroscopy and mass spectrometry (Table 1).

2.4. Preparation of the catalyst precursors 17–32

Complexes **17–32** were synthesized via a 1:1 addition reaction. Compounds **1–16** were added to an iron(II) chloride solution in diethylether or diethylether/tetrahydrofuran (Fig. 3). The resulting complexes are paramagnetic and were characterized by elemental analyses and mass spectrometry (see Section 4).

2.5. Heterogeneous catalyst synthesis and ethene polymerization results

Heterogeneous metallocene catalysts are frequently formed by immobilizing the cocatalyst on the surface of a carrier material followed by addition of a homogeneous solution of the metallocene complex. The metallocene complex is simultaneously



- 1** (R = methyl, R' = H, R'' = H)
2 (R = methyl, R' = methyl, R'' = H)
3 (R = methyl, R' = methyl, R'' = H, X = methyl)
4 (R = methyl, R' = R'' = methyl)
5 (R = methyl, R' = R'' = X = methyl)
6 (R = methyl, R' = R'' = ethyl)
7 (R = methyl, R' = methyl, R'' = isopropyl)
8 (R = methyl, R' = R'' = isopropyl)

- 9** (R = methyl, R' = R'' = X = methyl, Y = Br)
10 (R = ethyl, R' = R'' = methyl)
11 (R = phenyl, R' = R'' = methyl)
12 (R = phenylethyl, R' = R'' = methyl)
13 (R = methyl, R' = isopropyl, R'' = H)
14 (R = methyl, R' = tert. butyl, R'' = H)
15 (R = methyl, R' = methyl, R'' = H, X = ethyl)
16 (R = methyl, R' = methyl, R'' = H, X = isopropyl)

Fig. 2. Synthesis of the diiminopyridine compounds **1–16**.

Table 1
NMR spectroscopic and mass spectrometric data of compounds 1–16

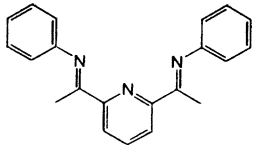
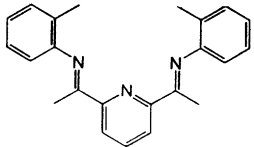
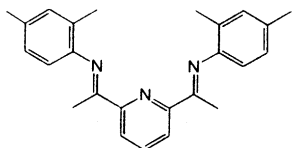
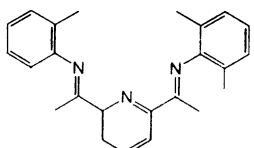
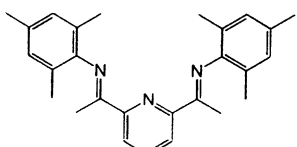
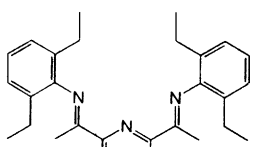
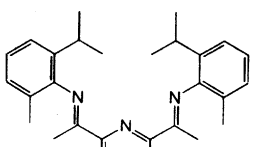
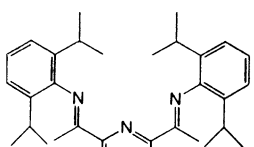
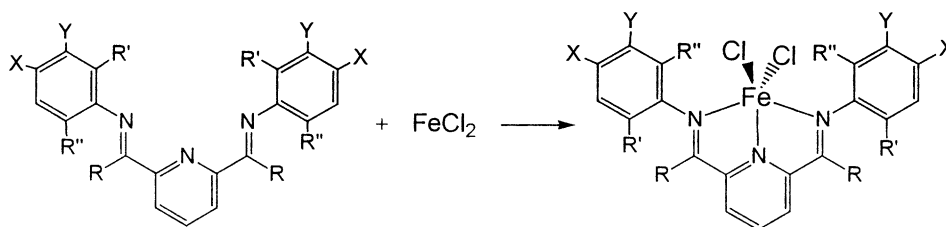
No.	Compound	^1H NMR ^a	^{13}C NMR ^b	MS, M^+ (m/e)
1		8.14 (d, 1H), 7.59 (t, 2H), 7.25–6.66 (m, 10H), 2.15 (s, 6H)	(C _q): 166.6, 160.8, 152.4 (CH): 138.7, 128.9, 124.1, 123.3, 119.7 (CH ₃): 16.5	n.d. ^c
2		8.13 (d, 1H), 7.86 (t, 2H), 7.22–6.69 (m, 8H), 2.31 (s, 6H), 2.13 (s, 6H)	(C _q): 164.6, 154.7, 148.7, 133.1 (CH): 138.5, 130.1, 125.5, 124.3, 123.2, 118.4 (CH ₃): 18.0, 16.4	341
3		8.38 (d, 1H), 7.86 (t, 2H), 7.04–6.56 (m, 6H), 2.32 (s, 12H), 2.09 (s, 6H)	(C _q): 166.9, 155.1, 147.4, 132.9, 127.1 (CH): 136.7, 131.1, 126.9, 122.1, 118.1 (CH ₃): 20.8, 17.7, 16.2	369
4		8.23 (d, 1H), 7.86 (t, 2H), 7.04–6.52 (m, 6H), 2.35 (s, 12H), 2.13 (s, 6H)	(C _q): 167.2, 155.1, 148.7, 136.4, 125.4, 122.2 (CH): 127.9, 123.0 (CH ₃): 18.0, 16.5	369
5		8.36 (d, 1H), 7.88 (t, 2H), 6.95–6.75 (m, 6H), 2.32 (d, 18H), 1.90 (s, 6H)	(C _q): 167.4, 155.2, 146.2, 132.2, 125.3 (CH): 136.8, 128.5, 122.1 (CH ₃): 20.7, 17.9, 16.4	397
6		8.36 (d, 1H), 7.90 (t, 2H), 7.12–6.70 (m, 4H), 2.63–2.25 (m, 8H), 2.22 (s, 6H), 1.22–1.05 (m, 12H)	(C _q): 166.9, 155.1, 136.9 (CH): 147.8, 131.2, 127.7, 126.0, 125.9, 123.3, 122.2, (CH ₂): 24.6, 24.3 (CH ₃): 16.8, 13.8, 13.0	425
7		7.82 (d, 1H), 7.18 (d, 2H), 6.98–6.76 (m, 6H), 2.85 (sept, 2H), 2.14 (s, 6H), 1.96 (s, 6H), 1.21 (dd, 12H)	(C _q): 167.1, 155.2, 147.6, 136.2, 125.0 (CH): 138.4, 127.8, 123.2, 118.3, 28.3 (CH ₃): 23.1, 22.8, 18.1, 6.8	453
8		7.85 (d, 1H), 7.20 (d, 2H), 6.88–6.72 (m, 6H), 2.88 (sept, 4H), 2.12 (s, 6H), 1.20 (dd, 24H)	(C _q): 167.1, 158.2, 145.6, 138.2 (CH): 138.8, 125.8, 123.9, 122.4 (CH ₃): 26.1, 23.3, 16.6	481

Table 1 (Continued)

No.	Compound	^1H NMR ^a	^{13}C NMR ^b	MS, M^+ (m/e)
9		8.45 (d, 1H), 7.90 (t, 2H), 6.98 (d, 2H), 2.39 (s, 6H), 2.22 (s, 6H), 2.15 (s, 6H), 1.97 (s, 6H)	(C _q): 167.9, 154.8, 147.1, 132.2, 125.2, 124.0 (CH): 136.7, 129.5, 122.2 (CH ₃): 23.3, 18.3, 17.5, 16.4	556
10		8.38 (d, 1H), 7.85 (t, 2H), 7.03–6.80 (m, 6H), 2.75 (q, 4H), 1.98 (s, 12H), 1.44 (t, 6H)	(C _q): 171.4, 154.5, 148.4, 125.3 (CH): 127.9, 122.9 (CH ₂): 23.2 (CH ₃): 18.2, 11.3	397
11		8.32–8.27 (m, 6H), 7.60 (d, 2H), 7.50 (s, 4H), 7.01–6.88 (m, 6H), 1.98 (s, 12H)	(C _q): 165.9, 152.9, 149.1, 132.0, 126.9 (CH): 139.6, 130.9, 130.0, 128.6, 126.0, 124.8, 124.0, 122.8 (CH ₃): 17.5	n.d.
12		8.53 (d, 1H), 8.18–7.96 (m, 4H), 7.26–6.81 (m, 14H), 3.70–3.54 (m, 4H), 3.13–2.71 (m, 4H), 2.00 (s, 12H)	(C _q): 168.9, 154.9, 152.2, 141.0, 126.1 (CH): 137.6, 128.6, 128.5, 126.1, 125.0, 123.3, 122.8 (CH ₂): 29.7 (CH ₃): 18.1	549
13		8.14 (d, 1H), 7.59 (d, 2H), 7.26–6.67 (m, 8H), 3.00 (sept, 2H), 2.13 (s, 6H), 1.21 (d, 12H)	(C _q): 166.6, 155.5, 148.7, 138.1 (CH): 136.8, 126.1, 125.7, 124.0, 122.2, 118.4, 28.5 (CH ₃): 22.8, 16.4	397
14		8.14 (d, 1H), 7.59 (d, 2H), 7.19–6.80 (m, 8H), 2.11 (s, 6H), 1.18 (s, 18H)	(C _q): 170.2, 158.5, 148.2, 139.0, 35.5 (CH): 138.0, 128.4, 125.3, 124.0, 123.8, 123.1 (CH ₃): 31.2, 16.2	425
15		8.16 (d, 1H), 7.64 (d, 2H), 6.97–6.80 (m, 4H), 6.40 (m, 2H), 2.70 (q, 4H), 2.10 (s, 6H), 2.08 (s, 6H), 1.40 (t, 6H)	(C _q): 166.9, 159.1, 152.5, 139.5, 128.9 (CH): 138.0, 130.9, 130.0, 124.8 (CH ₂): 28.0 (CH ₃): 18.8, 16.6, 15.7	397
16		8.14 (d, 1H), 7.60 (d, 2H), 7.16–6.61 (m, 6H), 2.85 (sept, 2H), 2.28 (s, 6H), 2.10 (s, 6H), 1.25 (d, 12H)	(C _q): 167.1, 155.2, 147.6, 136.1, 125.0 (CH): 136.9, 127.8, 123.3, 123.3, 122.2, 28.4 (CH ₃): 23.1, 22.9, 18.2, 16.8	425

^a 25°C, in chloroform-*d*₁, δ (ppm) rel. chloroform (7.24).^b 25°C, in chloroform-*d*₁, δ (ppm) rel. chloroform-*d*₁ (77.0).^c n.d. = not determined.



- 17** (R = methyl, R', R'' = H)
18 (R = methyl, R' = methyl, R'' = H)
19 (R = methyl, R', X = methyl, R'' = H)
20 (R = methyl, R', R'' = methyl)
21 (R = methyl, R', R'', X = methyl)
22 (R = methyl, R', R'' = ethyl)
23 (R = methyl, R' = methyl, R'' = isopropyl)
24 (R = methyl, R', R'' = isopropyl)
25 (R = methyl, R', R'', X = methyl, Y = Br)
26 (R = ethyl, R', R'' = methyl)
27 (R = phenyl, R', R'' = methyl)
28 (R = phenylethyl, R', R'' = methyl)
29 (R = methyl, R' = isopropyl, R'' = H)
30 (R = methyl, R' = tert. butyl, R'' = H)
31 (R = methyl, R' = methyl, R'' = H, X = ethyl)
32 (R = methyl, R' = isopropyl, R'' = H, X = methyl)

Fig. 3. Synthesis of the catalyst precursors 17–32.

activated and attached to the surface of the carrier. Several patents and articles have been issued in recent years that describe the heterogenization of MAO and various catalyst precursors on a carrier material [16–19]. Supporting catalyst precursor **20** on Witco prepared HL/04 silica-supported MAO (Al/Fe molar ratio = 253/1) produced a catalyst with an activity of less than 500 g PE/g_{cat} h.

Due to the very low activity of the heterogeneous Fe/MAO catalyst, other methods of forming analogous heterogeneous catalysts were tried. The method producing the best results was the PHT method described previously [7]. The addition of water to TMA in the presence of dried silica was shown to produce a significantly different heterogeneous support than if TMA was added to wet silica. At the equivalent Al/Fe molar ratio and reactor conditions to those used for the Fe(II)/MAO system described above, the PHT method produced a catalyst that was 30 times more active (10,200 g PE/g_{cat} h).

For the PHT method, the carrier material used was calcined silica with a water content of <1.2 wt.%. The silica was suspended in toluene and treated with TMA.

Then the desired amount of water was added to form the PHT. Addition of the selected catalyst precursor **17–32** yielded the active heterogeneous ethene polymerization catalyst (Fig. 4). Using this method, the water to aluminum content can be varied over a broad range. The location and nature of substituents on the diiminopyridine ligand were highly influential in determining the catalytic activity of the activated complex as well as observed properties.

2.5.1. Different aluminum/iron molar ratios

The activities of heterogeneous PHT/metallocene catalysts are dependent on the aluminum/transition metal molar ratios. In an earlier study [7] with a metallocene catalyst, the maximum activity was observed at an Al/Zr molar ratio of about 260/1. Even slight deviations in the Al/Zr molar ratio were found to dramatically alter the activity. At molar ratios under 50/1, the polymerization system exhibited almost no activity.

In contrast, the heterogeneous iron containing catalysts exhibit high activities even at low Al/Fe molar ratios, 8/1, as shown in Table 2 and Fig. 5. Molar ratios lower than 8/1 were not tested as the

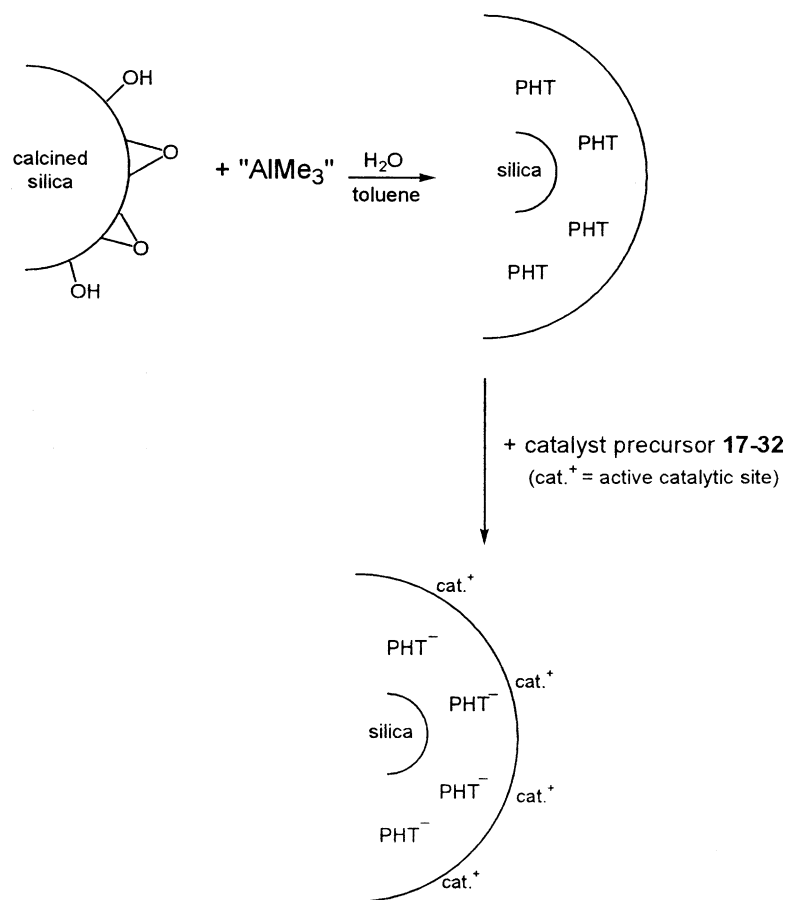


Fig. 4. Synthesis of a PHT-supported catalyst.

Table 2
Activity as a function of Al/Fe molar ratios

Al/Fe molar ratio, catalyst precursor 20 + PHT	Activity (g PE/g _{cat} h) ^a	Activity (g PE/g _{Fe} h)
8	55740	920000
21	27860	1030000
43	17860	1100000
84	25600	2930000
170	11500	2890000
254	10200	4380000
339	2460	1290000
509	1570	155000

^a The cat = catalyst precursor **20** on PHT.

catalyst precursor was not entirely immobilized under these conditions. As expected, no catalytic activity was observed for any of the iron(II) complexes studied in the absence of a cocatalyst.

Activities, based on g PE/g_{Fe} h, go through a maximum at an Al/Fe molar ratio of about 220/1 (Fig. 5). The activities are comparable to those observed for many metallocene catalysts ([20–23] and references therein).

2.5.2. Varying water/aluminum molar ratios

One of the most surprising observations regarding iron/PHT olefin polymerization catalysts is that water to aluminum molar ratios over 1.0 result in the highest activities. In contrast, metallocene/PHT catalysts frequently show their highest activities at a water/Al molar ratio of 0.69 [7,24] and half-sandwich imino complexes/PHT at a molar ratio of 0.83 [25].

Theoretical and mechanistic studies suggest that MAO, of which 20–30% of the aluminum is present as 'free' TMA, methylates the metallocene dichloride

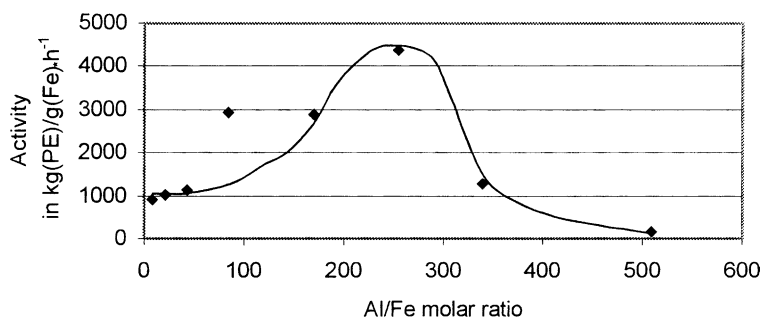


Fig. 5. Molar ratios Al/Fe vs. activity (g PE/g_{Fe} h). Catalyst precursor **20** on PHT. Polymerization conditions: H₂O/Al molar ratio = 0.93; 31 bar ethene pressure at 90 °C in isobutane; 8.5 mmol hydrogen added at the start of the polymerization runs; 60 min polymerization time.

complex prior to any catalytic activity. After methylation, one methyl anion is abstracted. The metallocene mono methyl cation formed is thought to be the active species ([26–34] and references therein).

In contrast, the PHT activated iron containing catalysts show little activity at water/Al molar ratios similar to those found in conventional MAO. Instead, these catalysts are most active at a water/aluminum molar ratio of 1.1 (Fig. 6). At this molar ratio it is unlikely that free TMA still exists. This suggests that free TMA is not needed to activate these complexes and that free TMA may reduce activity for the iron catalysts studied. Activities drop to zero when the water/aluminum molar ratio exceeds 1.5 as expected. At this point there

should be few remaining aluminum–methyl bonds and very little if any ‘free TMA’.

Therefore, it is possible that any aluminum–methyl bond is capable of activating selected iron(II) chloride complexes and thus initiating the polymerization reaction. Each type catalyst precursor, activated with PHT, may require a different water/Al molar ratio to obtain its best catalytic activity. The reason for such behavior might result from the fact that late transition metals, e.g. iron, cobalt or nickel are less oxophilic than titanium, zirconium or hafnium and more robust against typical Lewis base poisons. Thus, higher water/transition metal molar ratios in the catalyst may have less effect on the late than early transition

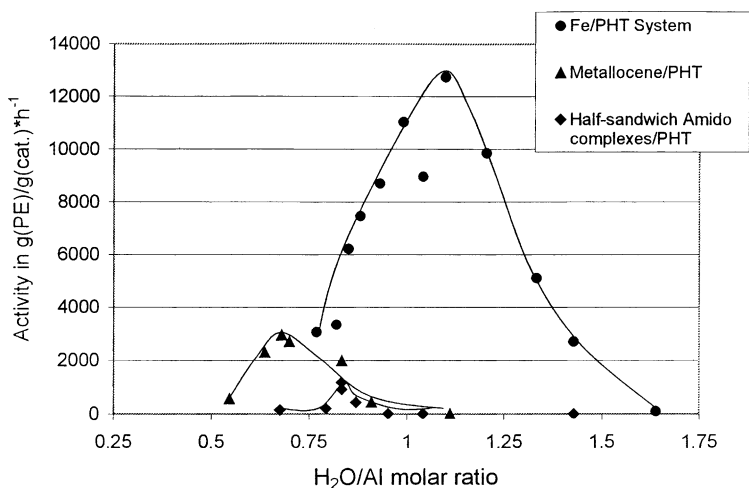


Fig. 6. H₂O/Al molar ratio vs. catalyst activity (g PE/g_{cat} h). Catalyst precursor **20** on PHT. Polymerization conditions: Al/Fe molar ratio = 253/1; Al/Zr molar ratio 260/1; 31 bar ethene pressure at 90 °C in isobutane; 8.5 mmol hydrogen added at the start of the polymerization runs; 60 min polymerization time.

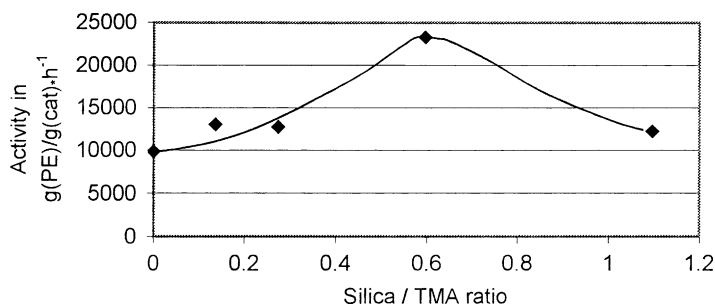


Fig. 7. Activity vs. silica/trimethylaluminum weight ratio. Catalyst precursor **20** on PHT. Polymerization conditions: H₂O/Al molar ratio = 1.1/1; Al/Fe molar ratio = 253/1; 31 bar ethene pressure at 90 °C in isobutane; 8.5 mmol hydrogen added at the start of the polymerization runs; 60 min polymerization time.

metal/PHT catalysts. Likewise, it may also be that an alternative activation mechanism or anion/cation equilibrium exists. Further investigations are necessary to discern the reasons for the observed behavior.

2.5.3. Varying aluminum/silica molar ratios

In order to prepare a PHT/metallocene catalyst system, a carrier, such as silica, is generally used to prevent reactor fouling. For the studies reported here, Davison XPO 2410, a calcined silica containing less than 1.2 wt.% total volatiles at 955 °C, was selected. The activity of the catalyst was influenced by the silica to TMA weight ratio (see Fig. 7). The degree of fouling is dependent on the silica content of the final catalyst [7,24]. The iron(II) dichloride/PHT system showed no reactor fouling tendency even if no support material was incorporated. Under these conditions, the obtained

solid could be used as a heterogeneous catalyst. Its polymerization behavior was comparable to other investigated catalyst systems.

2.5.4. Influence of hydrogen and comonomers during polymerization

Most ethene polymerizations were carried out in the presence of hydrogen, and some were carried out in the presence of both hydrogen and 1-hexene. Under the chosen polymerization conditions, almost no activity was observed in the absence of hydrogen. Traces of hydrogen greatly improved activity (Fig. 8), but further increases in hydrogen concentration decreased activity. Addition of 1-hexene at constant ethene concentration results in a decrease in activity (Fig. 9). However, when the polymers were analyzed by ¹³C HT-NMR spectroscopy, no incorporation of 1-hexene was found.

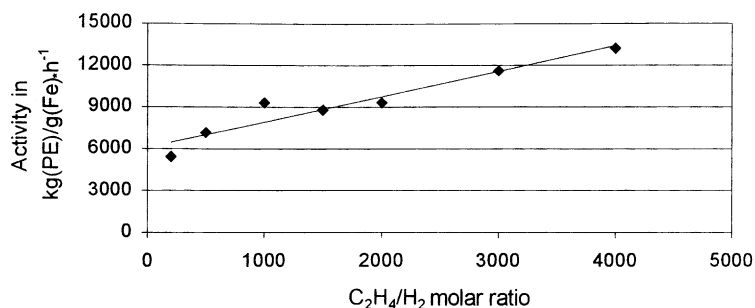


Fig. 8. Increasing activity with decreasing hydrogen concentration at constant ethene concentration. Catalyst precursor **20** on PHT. Polymerization conditions: Al/Fe molar ratio = 253/1; H₂O/Al molar ratio = 1.15/1; 31 bar ethene pressure at 90 °C in isobutane; 60 min polymerization time.

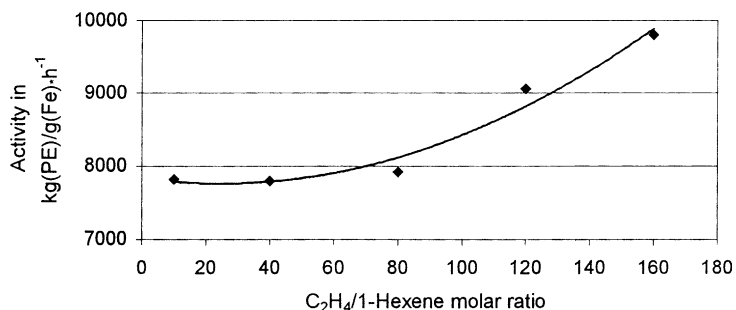


Fig. 9. Influence of 1-hexene on the activity of catalyst precursor **20** on PHT. Polymerization conditions: Al/Fe molar ratio = 253/1; H₂O/Al molar ratio = 1.15/1; 31 bar ethene pressure at 80°C in isobutane; 8.5 mmol hydrogen and 1-hexene fed continuously during polymerization; 60 min polymerization time.

2.5.5. Influence of reactor residence time on polymerization behavior

Activity was found to be directly related to the reactor residence time (Fig. 10). No decline in activity was noted with run length. This kinetic profile suggests that the catalytically active polymerization centers do not decay over the time frame of the experiments. In contrast, most metallocene complexes lose activity rapidly when the run length increases. It is likely that traces of oxygen and water fed with the ethene into the reactor affect those catalytic centers negatively. Unlike metallocenes, the Fe/PHT system may benefit from those impurities.

2.5.6. Steric and electronic effects on catalyst activity

Polymerization reaction kinetics are influenced by both steric and electronic changes at the transition metal catalytic center. Such changes occur when various functional groups are substituted onto either the aniline moiety or onto the carbon atom at the imino moiety.

The activity decreases with the increasing bulk of substituents in the 2- and 6-positions of the anilines: dimethyl > diethyl > methyl-isopropyl > diisopropyl (Fig. 11). Activity can be increased as much as 42% by substituting the 2,6-dimethyl aniline moiety with a 3-bromo-2,4,6-trimethyl aniline moiety (Fig. 12).

The steric and electronic effects of substituents on the transition metal polymerization site also influence the nature of the polymers produced. Low molecular weight, waxy polymers ($\bar{M}_w = 2700$ g/mol) are produced with catalysts that are only substituted in the 2-position of the aniline moieties. In contrast, substitution at both the 2- and 6-positions produces high molecular weight polymers MI = 0.1 dg/min; $\bar{M}_w = 455,000$ g/mol. These results are in agreement with the work first reported by Brookhart and coworkers [1].

It is important to note that both the melt index (MI) and high load melt index (HLMI) data are dependent on the polymerization run length. Additional or other

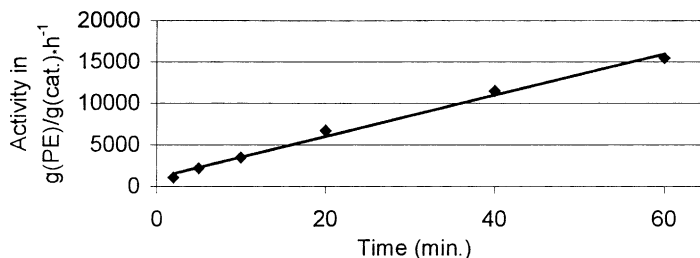


Fig. 10. Polymerization run-time vs. activity. Catalyst precursor **20** on PHT. Polymerization conditions: Al/Fe molar ratio = 253/1; H₂O/Al molar ratio = 1.15/1; 31 bar ethene pressure at 90°C in isobutane; 8.5 mmol hydrogen added at the start of the polymerization runs.

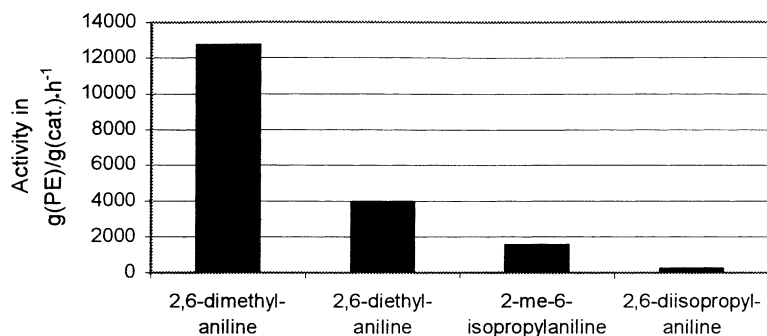


Fig. 11. Influence of increasing substituent bulkiness on activities. Catalyst precursors **20–23** on PHT. Polymerization conditions: Al/Fe molar ratio = 253/1; H₂O/Al molar ratio = 1.15/1; 31 bar ethene pressure at 90 °C in isobutane; 8.5 mmol hydrogen added at the start of the polymerization runs; 60 min polymerization time.

functional groups on the aniline rings have almost no influence on the molecular weights of the obtained polymers (Fig. 13).

The impact of imino substituents at the imino moiety on resin properties are much less pronounced. Only a small decrease in molecular weight is observed as the bulk of the substituent is increased (Table 3).

2.5.7. Other support materials ('double shell' PHT)

Using the PHT technique in the absence of a carrier, a TMA solution in toluene was partly hydrolyzed in a water to aluminum molar ratio of 1.53. The fact that the solid was still pyrophoric following the water treatment indicates that not all aluminum–methyl groups were deactivated. Subse-

Table 3

Influence of different imino substituents on polymer properties

Imino substituent	MI (dg/min)	HLMI (dg/min)	HLMI/MI
Methyl	0.1	2.31	23.1
Ethyl	0.24	27.00	112.5
Phenyl	0.01	3.72	372.0
Phenylethyl	0.02	n.a.	n.a.

quently, the solid product obtained was then used as the carrier material in another PHT preparation ('double shell'). In the second step, a water to aluminum molar ratio of 1.15 was used. The catalyst precursor was only added after the second preparation step

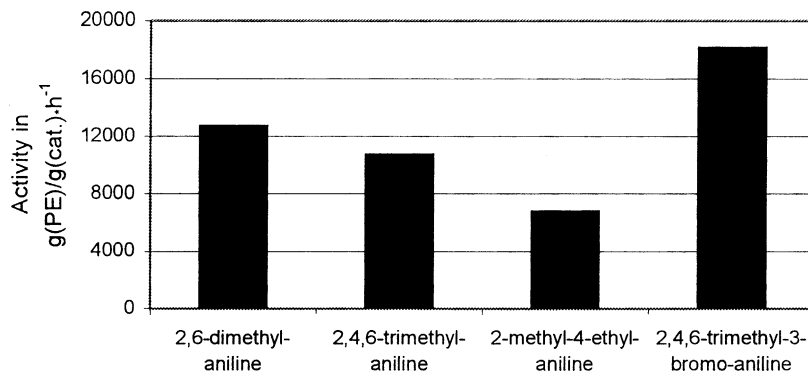


Fig. 12. Influence of different substitution patterns on the aniline moiety of the iron containing catalyst precursors on activity. Catalyst precursors **20, 19, 25, 22** on PHT. Polymerization conditions: Al/Fe molar ratio = 253/1; H₂O/Al molar ratio = 1.15/1; 31 bar ethene pressure at 90 °C in isobutane; 8.5 mmol hydrogen added at the start of the polymerization runs; 60 min polymerization time.

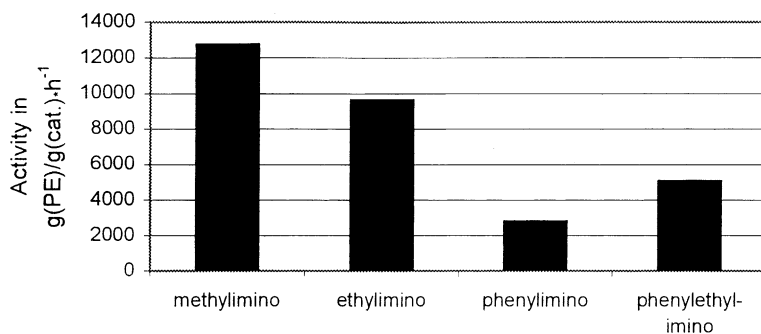


Fig. 13. Influence of various bulky substituents at the imino moiety on activity. Catalyst precursor **20**, **26**, **27**, **28** on PHT. Polymerization conditions: Al/Fe molar ratio = 253/1; H₂O/Al molar ratio = 1.15/1; 31 bar ethene pressure at 90 °C in isobutane; 8.5 mmol hydrogen added at the start of the polymerization runs; 60 min polymerization time.

(Fig. 14). The PHT ‘double shell’ catalyst was 35% more active than the normal PHT catalyst (20,000 versus 13,000 g PE/g_{cat} h, respectively).

3. Polymer properties

The physical, mechanical and optical properties of polyolefins determine their utility and quality. The MI and HLMI of all obtained polyethenes were deter-

mined. In addition, other test methods, e.g. high temperature gel permeation chromatography, density and high temperature NMR, were conducted.

3.1. HT-GPC results

The molecular weights of polyethenes made with homogeneous (MAO) and heterogeneous (PHT) diiminopyridine iron(II) dichloride catalysts vary significantly. The polymer produced with the heterogeneous

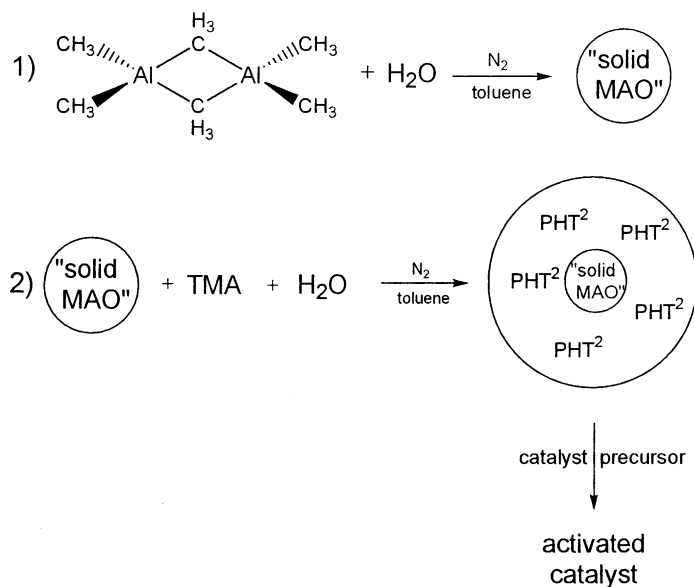


Fig. 14. Preparation of a ‘double shell’ PHT catalyst system.

Table 4

Comparison of molecular weights and molecular weight distributions of homogeneously and heterogeneously polymerized polyethenes made with catalyst **20**

	\bar{M}_n (g/mol)	\bar{M}_w (g/mol)	Polydispersity
Homogeneously polymerized PE	6700	91000	13.6
Heterogeneously polymerized PE	41000	412000	10.2

catalyst has a number average molecular weight six times higher than the polymer made with the homogeneous catalyst (see Table 4). Similarly, the weight average molecular weight is about four to five times higher for the hetero- versus the homopolymerized resin.

The molecular weight distribution of the heterogeneously polymerized resin is unexpectedly narrower than for the homogeneously polymerized resin. The HT-GPC curve for the homogeneously polymerized polyethylene indicates that this resin is bimodal while the similar curve for the heterogeneously polymerized polyethylene does not show any bimodal character (see Fig. 15). However, the heterogeneously polymerized polyethylene has a much broader molecular weight distribution than would be expected for a single site catalyst.

Unexpectedly, the weight average molecular weights of polyethenes made with a heterogeneous catalyst were observed to be run-time dependent. The resin obtained from a 2 min run had an \bar{M}_w of about 60 kg/mol while the resin from a 60 min run had an \bar{M}_w of 260 kg/mol. The plot in Fig. 16 illustrates the relationship between polymerization time and \bar{M}_w .

The molecular weight distribution of the resins, made at different residence times, is also dependent on the length of the polymerization. The polydispersity increases with time as seen in Fig. 16. The polymer from a 2 min run has a polydispersity of 5.1 while the polymer from a 60 min run broadens to a polydispersity of 12.4. The observed changes in the \bar{M}_w and polydispersity with polymerization time are difficult to explain on the basis of ethene diffusion limitations resulting from the growing fluff particles [28]. Rather

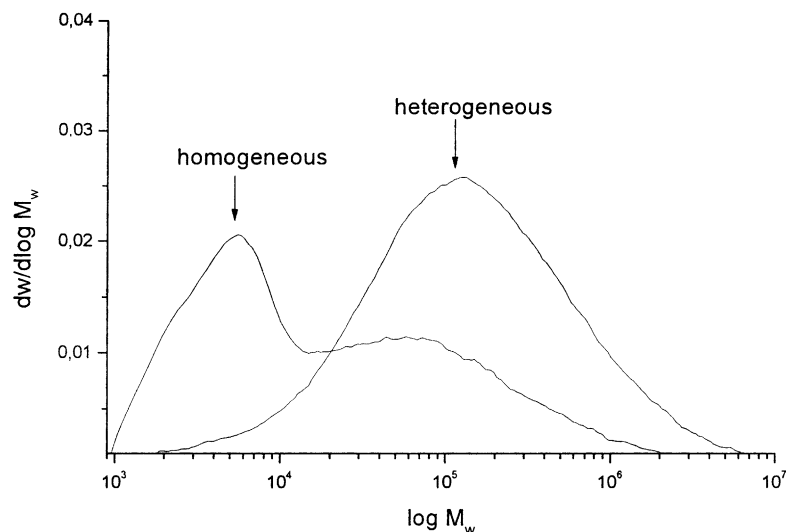


Fig. 15. Comparison of molecular weight distribution of homogeneously and heterogeneously obtained polyethenes. Catalyst: **20**/MAO. Polymerization conditions: Al/Fe molar ratio = 2000/1 (homogeneous) and **20**/PHT/silica; Al/Fe molar ratio = 253/1; H₂O/Al = molar ratio 1.15/1 (heterogeneous); 31 bar ethene pressure at 90 °C in isobutane; 8.5 mmol hydrogen added at the start of the polymerization runs; 60 min polymerization time.

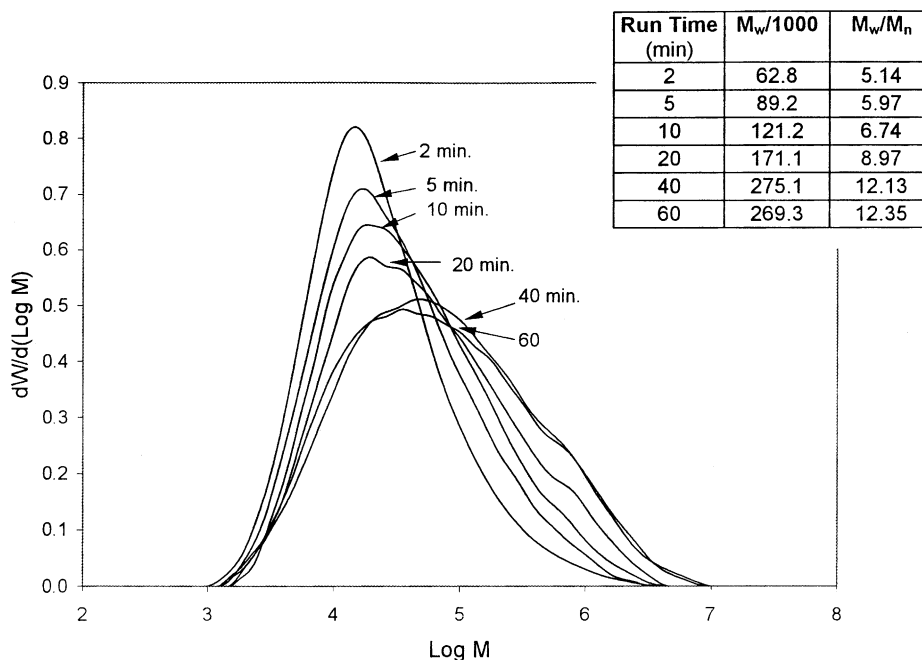


Fig. 16. Shifts of the molecular weight maxima with the polymerization time. Catalyst precursor **20** on PHT. Polymerization conditions: Al/Fe molar ratio = 253/1; H₂O/Al molar ratio = 1.15/1; 31 bar ethene pressure at 90 °C in isobutane; 8.5 mmol hydrogen added at the start of the polymerization runs; 60 min polymerization time.

it appears from the HT-GPC curves that there is a structure change of some of the active centers. As the polymerization proceeds, some of the active polymerization centers are changed such that they produce higher molecular weight polymers. At 20 min into a run one can see a distinct peak in the HT-GPC at $\log \bar{M}_w$ of about 5.8 that grows as the time increases and is not observed in resins from shorter run times. The nature of the polymerization site transformation is not currently understood, but such transformations are known to occur for metallocene catalysts as well [24].

Not only does the water/Al molar ratio influence the activity of the iron(II) complex/PHT system, but it also alters the molecular weight of the resulting resins as shown in Fig. 17.

As the water/Al molar ratio increased the molecular weight decreased linearly. No correspondence of activity with molecular weight was observed. The reason for the observed decrease in molecular weight with increasing water levels is clearly a reflection of the changing nature of the polymerization sites, but with-

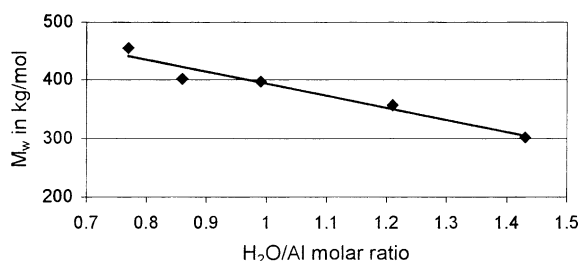


Fig. 17. Effect of water/Al molar ratio on the molecular weight of the obtained resin. Catalyst precursor **20** on PHT. Polymerization conditions: Al/Fe molar ratio = 253/1; 31 bar ethene pressure at 90 °C in isobutane; 8.5 mmol hydrogen added at the start of the polymerization runs; 60 min polymerization time.

out knowing the structure of these sites we cannot anticipate what these changes might be.

As described earlier, substituents can influence the molecular weight of the resulting polymer. Substituents in positions 2 and 6 or only in position 2 of the aniline moiety determine whether the resulting polymer is high or low in molecular weight.

Table 5

Influence of different substituents on the aniline part of the catalyst precursor on MI, HLMI, HLMI/MI data

Catalyst precursor	Substituent	MI (dg/min)	HLMI (dg/min)	HLMI/MI
20	2,6-Dimethyl	0.01	2.31	231
21	2,4,6-Trimethyl	0.03	3.9	130
25	3-Bromo-2,4,6-trimethyl	0.009	2.28	253

Table 6

Influence of different substituents on the imino part of the catalyst precursor on MI, HLMI, HLMI/MI data

Catalyst precursor	Substituent	MI (dg/min)	HLMI (dg/min)	HLMI/MI
20	Methyl	0.01	2.31	231
26	Ethyl	0.24	27	113
27	Phenyl	0.01	3.72	372
28	Phenylethyl	0.02	n.a.	n.a.

Substituents in other positions or different substituents on the aniline moiety do not influence the molecular weight significantly (Table 5).

Substituents at the imino moiety have little effect on resin molecular weight. Only the ethyl substituent significantly altered the resin molecular weight (Table 6).

3.2. Branching

As polymerization reaction time increases, the density of the resulting polyethene decreases (see Fig. 18). This decrease in density is not the result of short chain branch formation. Rather the density decrease is a reflection of the changes in the polymer molecular weight (see Fig. 19).

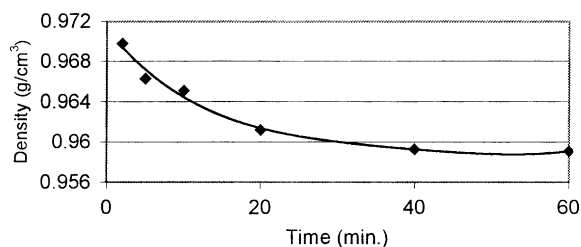


Fig. 18. Dependence of polyethene density on the polymerization time. Catalyst precursor **20** on PHT. Polymerization conditions: Al/Fe molar ratio = 253/1; H₂O/Al molar ratio = 1.15/1; 31 bar ethene pressure at 90 °C in isobutane; 8.5 mmol hydrogen added at the start of the polymerization runs.

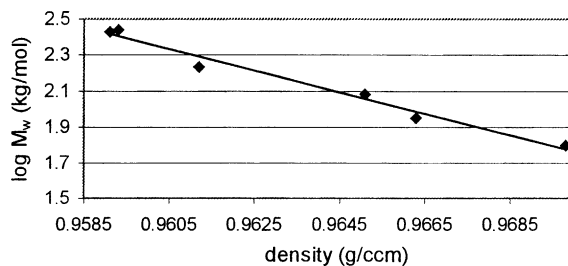


Fig. 19. Density of the polyethenes obtained at different run times vs. log \bar{M}_w . Catalyst precursor **20** on PHT. Polymerization conditions: Al/Fe molar ratio = 253/1; H₂O/Al molar ratio = 1.15/1; 31 bar ethene pressure at 90 °C in isobutane; 8.5 mmol hydrogen added at the start of the polymerization runs.

Even when 1-hexene was present during the polymerization run, the resulting polymer contained no detectable butyl branches by ¹³C HT-NMR spectroscopy.

4. Experimental

All procedures were performed under an inert gas atmosphere using standard Schlenk techniques or a glove box in order to eliminate traces of air or moisture. Purified and dried argon (BTS catalyst, molecular sieve) was used as the inert gas. All other preparations were carried out in air.

All solvents were purchased as technical grade purity and purified by distillation over Na/K alloy under argon atmosphere. All other chemicals were commercially available or were synthesized according to literature procedures.

NMR spectra were recorded in CDCl₃ at 25 °C on a Bruker ARX 250 instrument. The chemical shifts of ¹H NMR spectra were referenced to the residual proton signal of the solvent ($\delta = 7.24$ ppm for CHCl₃); the carbon resonances in ¹³C NMR spectra were also referenced to the solvent signal ($\delta = 77.0$ ppm for CDCl₃). Mass spectra were recorded on a Varian MAT CH7 instrument (direct inlet system, electron impact ionization 70 eV).

Polymer molecular weights were recorded on a Millipore Waters GPC 150C instrument. For the separation four successively connected polystyrene columns were used. The pore diameters of the single columns were 500, 1000, 10,000 and 100,000 Å. For the refractometric detection, a refractometer RI Waters 401 was used. The solvent was degassed 1,2,4-trichlorobenzene (flow rate of 1 ml/min). Polymer samples were dissolved in boiling 1,2,4-trichlorobenzene and filtered. The HT-GPC was calibrated with polystyrene standards. Polymerizations were conducted in isobutane at 90 °C and 31 bar ethene pressure for 1 h.

The MI is a measure of the amount of molten polymer that extrudes from an orifice under an applied pressure in a specific length of time. The HLMI is the same measurement but is 10 times the applied pressure. The measurements were made according to ASTM D1238 (conditions 190/2.16 and 190/21.6).

4.1. General procedure for the preparation of substituted diketopyridines

A Grignard reagent of bromoalkyl, bromoaryl or bromoalkylaryl compound was prepared. For this purpose a solution of 40 mmol of the bromo compound, dissolved in diethylether, was added dropwise to 0.97 g of magnesium (40 mmol) in diethylether. Next a solution of 2,6-dicyanopyridine (1 g = 7.74 mmol) in diethylether was prepared. Either the Grignard reagent was added dropwise to the stirred solution of 2,6-dicyanopyridine at 0 °C (inverse Grignard reaction) or the 2,6-dicyanopyridine was added dropwise to the stirred Grignard reagent at 0 °C (straight Grignard reaction).

The reaction products were monitored and controlled via GC/MS. After completion of the reaction, the mixture was hydrolyzed with diluted sulfuric acid (ca. 1 M) and the mixture was stirred for an additional 30 min.

Sodium carbonate was added carefully to the mixture until gas evolution stopped. The organic layer was separated, and the water layer was extracted twice with diethylether. The organic layers were combined, dried over Na₂SO₄ and evaporated to dryness. The residue was used without further purification.

4.2. General procedure for the preparation of the free ligands (condensation reaction)

To a stirred solution of the corresponding diketopyridine in toluene, 0.05 g of *p*-toluenesulfonic acid were added. The aniline compound was added in excess. The mixture was refluxed and the water formed was separated via a Dean–Stark trap. Refluxing was continued for 3–25 h (depending on the aniline used and/or the substituent at the diketopyridine). Completion of the reaction was determined via GC/MS.

After cooling to room temperature, the mixture was washed twice with a dilute solution of Na₂CO₃ in water and twice with water. The organic layer was separated and the water phase was extracted twice with diethylether. The combined organic layers were dried over Na₂SO₄ and evaporated to dryness. Ethanol was added to the dried residue. If crystallization did not start immediately, the solution was stored at –20 °C overnight.

The crystals were filtered off, washed with ethylalcohol and dried in air. The liquid residue was reduced in volume to about 30–40%. A second crop of crystals could be obtained after storing at –20 °C overnight. Overall yield: 90–95%.

4.3. General procedure for the preparation of the iron complexes 17–32

All complexes were prepared in an analogous manner. The corresponding diiminopyridine was stirred in a mixture of diethylether and tetrahydrofuran (1:1) at room temperature. Then one equivalent of finely powdered iron dichloride was added. A rapid color change indicated the reaction. Stirring was continued for at least 10 h. Then the colored solids were filtered,

Table 7

Mass spectrometric analysis (only highest mass peaks listed) and colors of the synthesized catalyst precursors

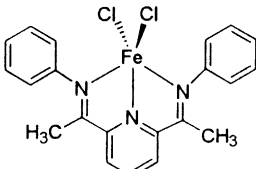
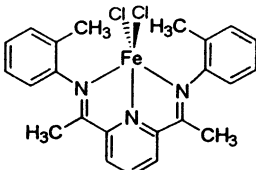
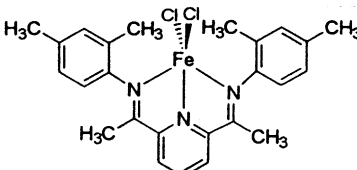
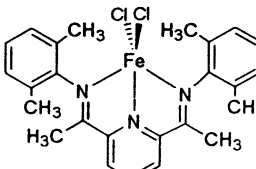
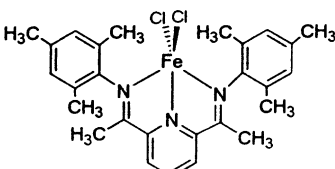
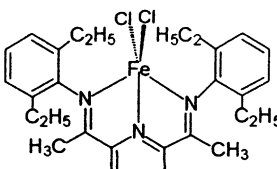
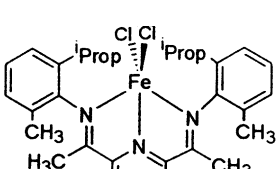
No.	Catalyst precursor	MS, M^+ (m/e)	Color
17		438	Black
18		467	Light blue
19		495	Blue
20		495	Blue
21		523	Blue
22		551	Blue
23		551	Light blue

Table 7 (Continued)

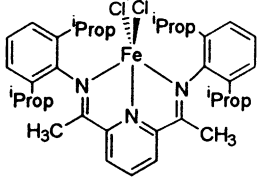
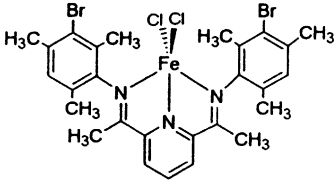
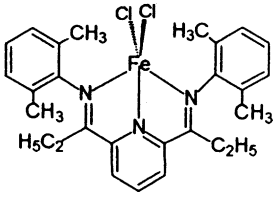
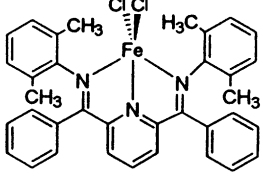
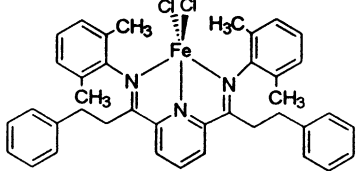
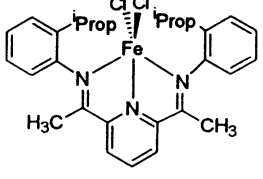
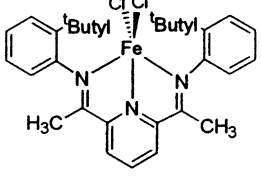
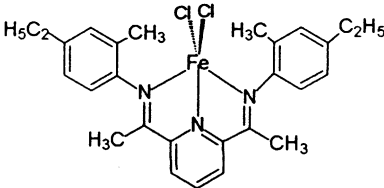
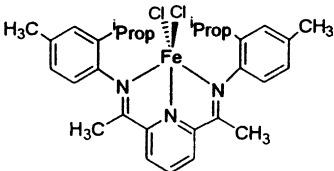
No.	Catalyst precursor	MS, M^+ (m/e)	Color
24		607	Blue
25		682	Dark blue
26		523	Blue
27		619	Blue
28		676	Light blue
29		524	Light blue
30		552	Dark green

Table 7 (Continued)

No.	Catalyst precursor	MS, M^+ (m/e)	Color
31		552	Blue
32		551	Blue

washed with diethylether and dried. The yields varied from 50 to 80% depending to what extent the solutions were used for crystallization.

4.4. Characterization of the catalyst precursors 17–32

The products **17–32** are paramagnetic and therefore NMR spectroscopy was not applied for characterization. Instead, elemental analyses (C, H, N, Cl) were performed for most derivatives in order to confirm the correct composition of the compounds. In addition, the mass spectra showed molecular ions for all derivatives (Tables 7 and 8).

4.5. General procedure for the preparation of a supported catalyst

To 1 g of dried Davison silica (XPO 2410) in a 500 ml Schlenk flask were added 100 ml of toluene

and 28.7 ml of a 1.764 M solution of TMA in toluene. The mixture was vigorously stirred for 30 min. Another flask containing 0.70 ml up to 1.5 ml of water was connected via a Teflon tube to the mixture and heated to 180 °C. The Teflon tube ended near the bottom of the reaction flask. Dry nitrogen was purged through the water containing flasks and a wet nitrogen stream was formed. This wet nitrogen stream transferred the vaporized water to the TMA/silica/toluene slurry. Purging continued until all the water was vaporized and transferred to the reaction flask. The slurry became highly viscous and the temperature increased to about 60 °C. Some toluene (ca. 50 ml) was added, and stirring was continued until the reaction flask had cooled down to room temperature. To the resulting slurry was added the iron(II) catalyst precursor (0.2 mmol), and stirring was continued for at least 1 h.

The slurry was filtered over a frit. After removing the toluene, the residue was washed with hexane and

Table 8
Elemental analyses

Complex	C _{Calc}	C _{Found}	H _{Calc}	H _{Found}	N _{Calc} (Cl _{Calc})	N _{Found} (Cl _{Found})
17	54.70	54.13	4.35	4.37	(16.11)	(16.10)
20	60.49	60.87	5.48	5.95	8.47	7.77
21	60.80	61.85	5.96	6.09	8.01	7.81
24	65.26	65.14	7.12	7.22	6.91	7.13
25	49.05	47.40	4.57	4.84	6.14	5.66
27	64.97	67.76	5.04	5.47	6.77	6.06
29	60.61	61.85	5.96	6.30	8.01	7.53
30	59.21	63.06	6.39	5.90	7.61	7.18

dried in vacuo to give a white solid. Overall yield was >95%.

Acknowledgements

We thank Witco company (Germany) for the donation of methylalumoxane.

References

- [1] B.L. Small, M. Brookhart, A.M.A. Bennett, *J. Am. Chem. Soc.* 120 (1998) 4049.
- [2] G.J.P. Britovsek, V.C. Gibson, B.S. Kimberley, P.J. Maddox, S.J. McTavish, G.A. Solan, A.J.P. White, D.J. Williams, *Chem. Commun.* (1998) 849.
- [3] G.J.P. Britovsek, V.C. Gibson, D.F. Wass, *Angew. Chem.* 111 (1999) 448.
- [4] G.J.P. Britovsek, V.C. Gibson, D.F. Wass, *Angew. Chem. Int. Ed. Engl.* 38 (1999) 428.
- [5] G.J.P. Britovsek, M. Bruce, V.C. Gibson, B.S. Kimberley, P.J. Maddox, S. Mastroianni, S.J. McTavish, C. Redshaw, G.A. Solan, S. Strömberg, A.J.P. White, D.J. Williams, *J. Am. Chem. Soc.* 121 (1999) 8728.
- [6] E.C. Alyea, P.H. Merrell, *Syn. React. Inorg. Chem.* 4 (1974) 535.
- [7] A. Köppl, H.G. Alt, S.J. Palackal, M.B. Welch, Phillips Petroleum Co., US Patent 5,900,035 (1999).
- [8] A. Andresen, H.G. Cordes, J. Herwiq, W. Kaminsky, A. Merck, R. Mottweiler, J. Pein, H. Sinn, H.J. Vollmer, *Angew. Chem.* 88 (1976) 889.
- [9] A. Andresen, H.-G. Cordes, J. Herwiq, W. Kaminsky, A. Merck, R. Mottweiler, J. Pein, H. Sinn, H.-J. Voilmer, *Angew. Chem. Int. Ed. Engl.* 15 (1976) 630.
- [10] H. Sinn, W. Kaminsky, *Adv. Organomet. Chem.* 18 (1980) 99.
- [11] H. Sinn, W. Kaminsky, H.-J. Vollmer, R. Woldt, BASF AG, US Patent 4,404,344 (1983).
- [12] G.F. Schmidt, D.A. Hucul, R.E. Campbell Jr., Dow Chemical Co., US Patent 5,015,749 (1991).
- [13] J.A.M. Canich, G.F. Licciardi, Exxon Chemical Co., US Patent 5,057,475 (1991).
- [14] T. Tsutsui, T. Ueda, Mitsui Petrochemical Ind., US Patent 5,234,878 (1993).
- [15] M. Chang, Exxon Chemical Co., US Patent 5,529,965 (1996).
- [16] O. Uchida, R. Sugimoto, Mitsu Toatsu Chemicals, Jpn. Kokai Tokyo Koko JP 04,234,405 [92,234,405] (1992); *Chem. Abstr.* 117 (1992) 2520034.
- [17] R. Jackson, J. Ruddelsden, D.J. Thompson, R. Whelan, *J. Organomet. Chem.* 125 (1977) 57.
- [18] W. Kaminsky, F. Renner, *Makromol. Chem. Rapid Commun.* 14 (1993) 239.
- [19] H.G. Alt, K. Patsidis, M.B. Welch, R.L. Geerts, B. Peifer, S.J. Palackal, D.R. Fahey, H.R. Deck, Phillips Petroleum Co., *Eur. Pat. Appl. Ep.* 628566 (1994); *Chem. Abstr.* 123 (1995) 33867.
- [20] K. Soga, T. Shiono, *Prog. Polym. Sci.* 22 (1997) 1503.
- [21] M. Bochmann, *J. Chem. Soc., Dalton Trans.* (1996) 255.
- [22] V.K. Gupta, S. Satish, I.S. Bhardwaj, *Rev. Macromol. Chem. Phys. C* 34 (1994) 439.
- [23] W. Kaminsky, *J. Chem. Soc., Dalton Trans.* (1998) 1413.
- [24] A. Köppl, H.G. Alt, M.D. Phillips, *J. Appl. Polym. Sci.* 80 (2001) 454.
- [25] A. Reb, Dissertation, Universität Bayreuth, 2000.
- [26] H.H. Brintzinger, D. Fischer, R. Müllhaupt, B. Rieger, R. Waymouth, *Angew. Chem.* 107 (1995) 1255.
- [27] H.H. Brintzinger, D. Fischer, R. Müllhaupt, B. Rieger, R. Waymouth, *Angew. Chem. Int. Ed. Engl.* 34 (1995) 1143.
- [28] G.G. Hlatky, H.W. Turner, R.R. Eckmann, *J. Am. Chem. Soc.* 111 (1989) 2728.
- [29] R. Taube, L. Krukowka, *J. Organomet. Chem.* 347 (1988) C9.
- [30] H. Schumann, D.F. Karasiak, S.H. Muhle, R.L. Haltermann, W. Kaminsky, U. Weingarten, *J. Organomet. Chem.* 579 (1/2) (1999) 356.
- [31] R.F. Jordan, C.S. Bajgur, W.E. Dasher, A.L. Rheingold, *Organometallics* 6 (1987) 1041.
- [32] J.J.W. Esthuis, Y.Y. Tan, J.H. Teuben, *J. Mol. Catal.* 62 (1990) 277.
- [33] L.A. Nekhaeva, G.N. Bondarenke, S.V. Ruykov, A.L. Nekhaev, B.A. Krentsel, V.P. Marin, L.I. Vyshinskaya, I.M. Khrapova, A.V. Polonskii, N.N. Korneev, *J. Organomet. Chem.* 406 (1991) 139.
- [34] H. Sinn, *Makromol. Chem., Makromol. Symp.* 97 (1995) 27.